Paleolakes and socioecological implications of last glacial "greening" of the South African interior

Andrew Carr, Brian Chase, Stephen Birkinshaw, Peter Holmes, Mulalo Rabumbulu, Brian Stewart

Final version available at: https://www.pnas.org/doi/10.1073/pnas.2221082120

Paleolakes and socioecological implications of last glacial "greening" of the South African interior

Andrew S. Carr*[1], Brian M. Chase*[2,3], Stephen J. Birkinshaw[4], Peter J. Holmes[5], Mulalo Rabumbulu[6], Brian A. Stewart*[7,8]

[1]School of Geography, Geology and the Environment, University of Leicester; Leicester LE1 7RH, UK.

[2]Institut des Sciences de L'Evolution-Montpellier (ISEM), University of Montpellier, Centre National de La Recherche Scientifique (CNRS), EPHE, IRD; 34095 Montpellier, France.

[3]Department of Environmental and Geographical Science, University of Cape Town; South Lane, Upper Campus, 7701 Rondebosch, South Africa.

[4]School of Engineering, Newcastle University; Newcastle upon Tyne NE1 7RU, UK.

[5]Department of Geography, University of the Free State; Bloemfontein 9300, South Africa.

[6]Department of Geography Environmental Management and Energy Studies, University of Johannesburg; Auckland Park 2006, South Africa.

[7]Department of Anthropology and Museum of Anthropological Archaeology, University of Michigan; Ann Arbor, MI 48109-1259.

[8]Rock Art Research Institute, University of the Witwatersrand; 2050 Wits, South Africa.

*Co-corresponding first authors: Andrew S. Carr, Brian M. Chase, Brian A. Stewart

Email: asc18@leicester.ac.uk; brian.chase@umontpellier.fr; bastew@umich.edu

Abstract

Determining the timing and drivers of Pleistocene hydrological change in the interior of South Africa is critical for testing hypotheses regarding the presence, dynamics and resilience of human populations. Combining geological data and physically-based distributed hydrological modelling, we demonstrate the presence of large paleolakes in South Africa's central interior during the last glacial period, and infer a regional-scale invigoration of hydrological networks, particularly during marine isotope stages (MIS) 3 and 2, most notably 55-39 ka and 34-31 ka. The resulting hydrological reconstructions further permit investigation of regional floral and fauna responses using a modern analogue approach. These suggest that the climate change required to sustain these water bodies would have replaced xeric shrubland with more productive, eutrophic grassland or higher grass-cover vegetation, capable of supporting a substantial increase in ungulate diversity and biomass. The existence of such resource-rich landscapes for protracted phases within the last glacial period likely exerted a recurrent draw on human societies, evidenced by extensive pan-side artifact assemblages. Thus, rather than representing a perennially uninhabited hinterland, the central interior's under-representation in late Pleistocene archeological narratives likely reflects taphonomic biases stemming from a dearth of rockshelters and regional geomorphic controls. These findings suggest that South Africa's central interior experienced greater climatic, ecological and cultural dynamism than previously appreciated, and potential to host human populations whose archaeological signatures deserve systematic investigation.

Significance

Renowned for its rich evidence pertaining to early *Homo sapiens*, South Africa's late Pleistocene archaeological record remains biased towards the continental margins. A profusion of coastal rockshelters, together with putative associations of glacial periods with intense aridity in the continental interior, has created historical impressions of an inland core hostile to human life during lengthy glacial phases. New geological data and large-scale hydrological modelling experiments reveal that a series of large, now-dry palaeolakes existed for protracted phases of marine isotope stages 3 and 2. Modern analogue reconstructions of resulting vegetational and faunal communities suggest glacial climates were capable of transforming South Africa's central interior into a resource-rich landscape favorable to human populations.

Main Text

Introduction

South Africa's archaeological record is world-renowned for a diversity of evidence relating to early *Homo sapien* lifeways (1). This record is biased towards the continental margins (Fig. 1), due partly to the favorable formation and preservation of rockshelters in such locales. Combined with historical assumptions concerning aridity-driven inhospitality of the continental interior, this has contributed to an emphasis on the significance of coastal regions for early modern human populations (e.g. 2, 3-9), with the southern Cape's now-submerged coastal platform posited as a glacial-phase refugium (6-8). *Sensu lato*, southern Africa's currently semi-arid interior basins are climatically and ecologically complex. Portions of them clearly experienced conditions amenable to human settlement at various times during the middle and late Pleistocene, as demonstrated by recent work in, for example, the northern and southern Kalahari (10-13), the Northern Cape (14), the Tankwa Karoo (15) and the eastern Free State (16). However, the precise timing and nature of environmental changes in South Africa's central interior (Fig. 1) – the semi-arid zone nearest the rich and well-studied southern Cape archaeological records – remain largely obscure, as does nature of the attendant resources that drew hunter-gatherers to it. Given these uncertainties, the effects of middle and late Pleistocene climate variability on human migration, dispersal and adaptation – in southern Africa as elsewhere – are subjects of ongoing debate (17, 18).

Key aspects of this debate can be informed by an improved understanding of the evolution of surface water systems (10, 19). Specifically, endoreic paleolake systems are sensitive indicators of precipitation-evaporation balance (e.g. 20, 21), and thus particularly amenable to integration with hydrological and paleoclimatic models (e.g. 22). In the central interior of South Africa, such paleolake basins (pans and playas) – often with rich assemblages of Middle and Later Stone Age (MSA and LSA) archaeological materials – have been described (14, 23-25). However, their geochronologies and climatic significance remain very poorly constrained. To redress this, we present a suite of new luminescence ages (n=23) and radiocarbon dates (n=18), which together with field mapping provides fresh perspectives on the timings of lacustrine phases in the central interior. We evaluate the significance of these data using a physically-based distributed hydrological model applied to the wider Orange River basin, which enables the reconstruction of regional paleohydrological and paleoecological conditions. Results indicate that during the last glacial period, for extended periods of MIS 3 in particular, the South African central interior was a potentially resource-rich landscape that would have been attractive to Pleistocene hunter-gatherer populations.

Results and Discussion

For this study, we investigated several pans across the South African interior (Fig. 1). The most extensive suite of unequivocal lacustrine deposits is preserved at Swartkolkvloer, a large pan (~70

km^2, 921 m a.s.l.) south of Brandvlei (Fig. 1, 2, SI p.9). Shorelines – at 11 m and 18 m above the modern pan floor – are located on the pan's southern and eastern margin at Breek Been Kolk (BBK; 14) and "Locality A" (23), while lagoonal sediments at +13 m were observed at the "Quarry". These deposits comprise a mixture of lacustrine marls, abundant shells of the aquatic gastropod *Tomichia ventricosa* and water-rolled gravels (23). Together, they indicate that a ~215 km^2 lake was present for sustained periods (Fig. 2). Luminescence and radiocarbon dating (n=19) indicate lacustrine phases from ~39±3 to 55±3 ka (939 m, +18 m) and from 31.4±0.3 to 34.4±0.7 cal kBP (932 m, +11 m), with a later, perhaps more ephemeral, phase potentially indicated by OSL dated lacustrine sediments (17±2 ka) and by previously reported *T. ventricosa* radiocarbon dates at BBK (14) (Fig. 2, SI p.12). Broadly consistent with these ages is the observation of a MSA non-centripetal lineal Levallois core on the 932 m Locality A shoreline, as well as MSA artifacts at adjacent Hoek van Spruit se Vloer. The latter matches descriptions of Sampson's (26) later Orangian Industry, dated to MSA 3 at Driekoppen (27) (SI p.22, 25). Stable isotope analyses of *T. ventricosa* shells (SI p.26) reveal strong $\delta^{13}C$ and $\delta^{18}O$ covariance, consistent with a closed lake basin environment (28). The lowest $\delta^{13}C$ and $\delta^{18}O$ values, indicative of the least evaporative conditions, were observed for specimens from BBK and the +18 m lake level.

Approximately 100 km north of Swartkolkvloer, *Unio caffer* shells from pan fill sediments at Grootvloer were radiocarbon dated to 20.7±0.2 and 21.7±0.6 cal kBP (SI). *U. caffer,* absent from this region today, requires perennial freshwater and the presence of fish to reproduce (29). Subjacent pan fill produced similar luminescence ages across three locations (20±1 to 24±2 ka; n = 3; SI p.35), indicating a lacustrine phase during the Last Glacial Maximum. A pan-margin artifact scatter rich in high-quality bladelets, bladelet and bipolar cores, and weathered ostrich eggshell provides evidence of a contemporary (early Robberg) human presence (SI p.37).

500 km to the northeast at Alexandersfontein, lacustrine beds 14.5 m above the modern pan floor (see 24) were radiocarbon dated to between 25.7±0.7 and 32.3±0.7 cal kBP. The minimum age of these beds is constrained by early Holocene luminescence ages from the overlying colluvium (9-10 ka). MSA lithic artifacts occur as a discontinuous, low-density scatter on the surfaces of the exposed lacustrine beds and at the base of the gullies formed within these beds. We estimate a ~35 km^2 lake associated with this water depth, compared with the ~44 km^2 19 m deep lake previously inferred to have developed during the LGM at 19.3±0.7 cal kBP (24). Evidence for such a 19 m high stand could not be (re)located (see SI discussion p.39). At a second site, Mauritzfontein, on the southern margin of the Alexandersfontein basin and ~10 m above the modern pan floor, late MIS 2 (13±1 ka) lacustrine marls overlie evidence for a lower MIS 3-2 lake phase (tentatively ~41 ka; SI p.46), the latter comprising a wave-cut calcrete and beach sands with *in-situ* MSA artifacts (24, 30).

To contextualize these data, we used the Shetran physically-based distributed hydrological model (31) to: 1) determine the conditions necessary to establish and maintain lake high-stands at Swarkolkvloer and Alexandersfontein, and 2) to estimate the resulting regional-scale hydrological rejuvenation of the wider Orange and Vaal river basins (Fig. 1). While we are not able to consider the impact of changes in the magnitude and frequency of rainfall events on water balance during the study period, results nonetheless indicate that to sustain the observed lacustrine features, increases in precipitation (P): potential evapotranspiration (PET) ratios of 75% (+18 m lake at Swarkolkvloer) and 60% (+19 m lake at Alexandersfontein) are required (Table S9). Applying paleotemperature estimates for the lacustrine phases (see Materials and Methods), we calculate that PET at Swarkolkvloer and Alexandersfontein was 21% and 25% lower than present, respectively, and precipitation increased by ~215% at Swarkolkvloer (to 550 mm/yr) and 88% at Alexandersfontein (to 820 mm/yr), conditions that would have led to a wide-spread rejuvenation of hydrologic systems in the central interior of South Africa (SI p.56).

From these data we therefore infer substantial humidity increases were required to sustain perennial surface water in the South African central interior during MIS 3-2 (Fig. 2, 3). The regional significance of these observations is apparent when considered in broader palaeoclimatic context,

and in light of evidence of increased MIS 3 humidity and hydrologic activity at other locales in the interior (e.g. 12, 32, 33-35). These high lake phases post-date the region's eccentricity-modulated transition from low to high latitude forcing dominance at ~70 ka (36), and correspond to periods of Antarctic sea-ice expansion from ~58-16 ka (37; Fig. 2). The highest shoreline at Swarkolkvloer is coincident with the precession-induced sea-ice maximum from ~55-40 ka, implying that equatorward displacements of the westerly storm track and increased winter rainfall may have been instrumental in establishing sustained lacustrine phases. This mechanism may have operated in isolation, or as part of a more complex dynamic, wherein frontal systems were brought into more direct association with tropical lows – favored by increased austral summer insolation – to form composite synoptic systems (i.e. tropical-temperate troughs) (38, 39). Indeed, stable carbon isotope evidence from the tooth enamel of grazing ungulates at Equus Cave indicates a moderate increase in cool-growing season C_3 grasses during late MIS 3 and MIS 2 (40), implying that while winter rainfall likely increased, it did not dominate the regional rainfall regime. Phases of speleothem growth at nearby Wonderwerk (34) and Lobatse (41) caves (50-44 ka, 31-36 ka and 26-13 ka) correspond with the reconstructed lacustrine phases and, combined with data from Tswaing Crater, these suggest that tropical moisture sources also had significant influence, at least during MIS 3 (Fig. 2). In contrast, paleolake reconstructions from the Makgadikgadi Basin of the Kalahari show limited correspondence with lacustrine phases of the South African interior (21), implying distinct responses to global drivers of climate change, cautioning against the extrapolation of northern Kalahari data to define regional climate dynamics (e.g. 11).

While evidence for wetter last glacial conditions was reported as early as 1973 (24, 32), a paucity of data and minimal chronology led to generalized characterizations of the South African interior that equated lower temperatures with aridity (e.g. 3). In contrast, the MIS 3-2 climatic changes implied here would have fundamentally transformed the South African central interior, rejuvenating regional hydrologic networks and significantly changing regional vegetation and faunal resources. Using a modern analogue approach based on the climatic conditions inferred from the hydrological modelling, and the modern distributions of vegetation types (42) and large ungulate taxa (43), our hydro-ecological models imply that during lacustrine phases regional environments would have been much grassier. This vegetation would have been akin to the modern Highveld and Drakensberg Grassland bioregions, or, if increases in winter rainfall were considerable, akin to a high grass-cover shrubland (Fig. 3; SI p.61). A critical difference between modern bioregions and their MIS 2-3 climatic correlates is the edaphic contrast between the (presently) dry interior and humid uplands. While the Mesic Highveld and Drakensberg grasslands are characterized by leached soils and less palatable sourveld grasses, soils of the interior are relatively unleached, and, with increased humidity, are likely to have supported more palatable, eutrophic grasslands for which there are no direct analogues in southern Africa today (44-46). Low temperatures would have almost certainly excluded savanna bioregions (47), but woodland taxa would have likely developed in riparian and less fire-prone niches, creating a diverse vegetation mosaic. While proxy data from the interior is extremely limited, the available pollen data from Wonderwerk and Equus Cave are consistent with MIS 2-3 conditions being cooler and wetter than the Holocene, characterized by open, grassy vegetation with occasional trees (34, 48).

Faunal data from Equus Cave support these findings, with MIS 2-3 assemblages differing markedly from those of the Holocene (33). While several taxa from the Pleistocene layers are now extinct, there is no precise modern analogue for the Equus Cave faunal assemblages (43). Best-fit modern assemblages for the MIS 2-3 herbivores are found the Central Bushveld Savanna and Mesic Highveld Grasslands to the east (Fig. 3; SI p.67) (43, 44, 49). Today, these regions are substantially more humid than the Equus Cave region (Aridity index: 0.51±0.16 compared to 0.28±0.3)(50), and accordingly support a much greater herbivore biomass (10,900 kg/km^2 compared to 5700 kg/km^2) (43). Most significant is the MIS 2-3 presence of water dependent taxa such as hippopotamus, crocodile and lechwe at Equus Cave (33). The latter's (*Kobus leche*) distribution is tightly linked to extensive swamps and wetlands, with the nearest modern occurrence being the Okavango Delta 900 km to the north (SI p.68). This again implies a substantial change

in regional environments, with surface water occurrences not just along perennial river courses, but across the array of now-dry basins that characterize the landscape (Fig. 3), consistent with our hydrologic model and environmental reconstructions. These findings may be extended to other sites, such as Florisbad, where, despite poor chronologic control, hominin remains are associated with evidence for cool, moist grassy conditions (51) and similarly distinct fauna, including hippopotamus and lechwe (52).

Together these results imply that during portions of MIS 3 and 2 the South African central interior experienced hydrological conditions that contrast markedly with perceptions of a persistently arid and inhospitable hinterland (Fig. 2). Instead, the region appears to have enjoyed protracted phases of abundant surface water and subsistence biomass. This allows us to account for some long-standing observations regarding the region's faunal and vegetation records, which indicate a more diverse fauna occupying a grassier landscape (34, 48). That these changes are not correlated with palaeolake phases in the northern Kalahari (21) is particularly interesting as it further highlights the spatial diversity of environmental responses to broader changes in global boundary conditions.

These findings also speak to long-standing questions regarding Pleistocene climatic conditions and human occupation of the South African interior (2-4, 11, 53-56), particularly during MIS 3 and 2. Both MSA and LSA archaeological materials occur throughout our study region and more widely across the Karoo (e.g. 15, 55, 57). Often this is surficial and unstratified archaeology, but its ubiquity on and near the landforms we investigated across our broader study region (SI) supports Butzer's (58) contention that evidence for paleolake highstands associates closely with diagnostically MSA artifacts. Crucially, however, we demonstrate that the most prominent waterbodies formed not in MIS 5, as previously suspected by Butzer (58), but during MIS 3-2, a timeframe broadly consistent with the character of most lake-associated lithic scatters (SI). It follows that the region's under-represented archaeological record is more likely to be a product of preservation biases related to regional geologies and geomorphologies (a lack of rockshelters and deflated landscapes, respectively) than of limited resources for hunter-gatherers, particularly given the profound behavioral plasticity of Pleistocene *H. sapiens*' (59, 60). While the dearth of interior rockshelters precludes assessments of demographic trends, available dating for archaeological contexts in the region imply a recurrent human presence, with extensive MSA material at sites for which our hydrological modelling clearly predicts MIS 3/2 inundation.

Southern Africa during MIS 3 and 2 witnessed major cultural changes, including the piecemeal abandonment of MSA technological traditions (61), the widespread adoption of miniaturized tools and standardized LSA microliths (62), and the establishment of new modes and magnitudes of social networking (63). Many of these changes were likely linked to environmental trends via shifting resource potentialities and demographic responses. That the central interior enjoyed, at least at times, high effective rainfall, water availability and large ungulate-supporting grasslands enhances the likelihood that societies residing there played a role in these processes. Our findings also support evidence for potentially analogous ecological responses during earlier glacial stages – particularly MIS 6 (64), when expanded sea-ice extent coincided similarly with high austral summer insolation – and models invoking an inhospitable interior as a pretext for the existence of coastal refugia for early *H. sapiens* (e.g. 6-8) may require re-evaluation. For now, these findings join emerging insights from elsewhere in the interior (e.g. 10, 11, 12, 13, 16, 65, 66) in highlighting the need to work towards a more nuanced picture of spatiotemporal variability in climatic conditions and resource availability for middle and late Pleistocene foragers. To this end, future work in the central interior should aim to integrate hydrological data like those presented here with the region's rich archaeological record by identifying and taking advantage of opportunities to chronologically constrain the latter. Only then can we appreciate when, how and

the extent to which ancient societies took advantage of the considerable opportunities afforded by glacial-phase landscapes in the subcontinent's interior basins.

Materials and Methods

Elevations for sites and analyses were established using the Multi-Error-Removed Improved-Terrain digital elevation model (67).

Geochronology (SI p.3)

Samples of the lacustrine gastropod *Tomichia ventricosa* (Swartkolkvloer) and the freshwater bivalve *Unio caffer* (Grootvloer) were manually extracted from encapsulating sediments under a binocular microscope. They were vigorously cleaned in deionized water with an ultrasound bath and inspected to ensure no adhering sediment or cement were present. Where possible, whole shells of *T. ventricosa* were analyzed. Samples were submitted to the ^{14}C Chrono Centre at Queen's University Belfast (samples UB-) or to Beta Analytical (samples Beta-). Radiocarbon ages were calibrated using CALIB 8.1.0 (68) using the SHCal20 Southern Hemisphere calibration dataset (69). As it presently remains unquantified, no reservoir effect corrections were made. Results are summarized in Supplementary Material Appendix A.

Luminescence dating samples were obtained by hammering steel tubes into cleaned exposures or by using a Dormer sand augering system. Samples were prepared for coarse grain (range 90-250 μm) quartz and/or K-feldspar analysis following standard methods (70). Luminescence measurements on (2 mm) multi-grain aliquots were performed on a Risoe DA20 TL/OSL reader. For quartz stimulation was provided by blue LEDs (stimulation wavelength 470 nm) at 70% power (40 s at 125°C) with the resulting luminescence detected through a U-340 detection filter. For K-feldspar, stimulation was provided by IR diodes (wavelength 870 nm) with detection through Schott BG39 filters and Corning 7-59 filters (detection range 320-450 nm). Equivalent doses (D_e) were determined using mineral-specific variants of the Single Aliquot Regeneration (SAR) protocol (71, 72). These comprised 5-7 regeneration dose point sequences and included a repeat dose point and a zero-dose point. For K-feldspar, the post-IR IRSL method (73-75) was used. This comprised an initial stimulation at 50 °C followed by a second (post-IR) stimulation at 225°C ($pIRIR_{225}$) or 290°C ($pIRIR_{290}$). K-feldspar fading rates were measured using subsets of aliquots from the SAR measurements following Auclair et al. (76) and fading rates ($g\text{-}value_{2days}$) and any fading corrections were analysed in the "*Luminescence*" R Package (77). For both minerals, aliquots with recycling ratios (repeat dose points in the dose-response curve) outside 10% of unity, or recuperation (sensitivity-corrected zero dose L_x/T_x) >5% of the sensitivity-corrected natural signal (L_n/T_n) were removed prior to averaging of the D_e distributions. Dose-response curves were fitted with saturating exponential fits, with D_e uncertainties incorporating counting statistics, curve fitting uncertainties and a 1% systematic uncertainty (calculated with the Risoe *Analyst* software (Duller, 2007). The uncertainty in the final D_e estimates incorporates a beta source calibration uncertainty (3%).

Single grain quartz analyses employed a focused 532 nm Nd:YVO_4 solid state diode-pumped laser emitting at 532 nm, focused to a ~20 μm spot. Dose-response curves were fitted with saturating exponential fits in the *Analyst* software and their uncertainties included the addition of a 3% systematic instrumental uncertainty (determined following Jacobs et al. 78). Grains were rejected (e.g. 79) if: 1) the test dose signal was less than 3 sigma above background; 2) the relative test dose uncertainty was larger than 20%; 3) the recycling ratio or IR depletion ratios were inconsistent with unity at two sigma; 4) recuperation (zero dose L_x/T_x) was greater than 5% of L_n/T_n; 5) the dose-response curve did not grow with dose; 6) a finite D_e or D_e uncertainty could not be obtained due to saturation of the dose response curve, or a failure of the L_n/T_n measurement to intercept the dose response curve. Results are summarised in Appendix A.

Environmental dose rates were determined using elemental concentrations obtained via inductively coupled plasma mass spectrometry (ICP-MS; for U and Th) and ICP-OES (for K). External beta dose rates were further evaluated using GM beta counting) (80). For some samples (SI) *in situ* gamma spectrometry measurements were undertaken (81). U, Th and K concentrations were converted to annual dose rates following Guerin et al. (82), then corrected for grain size (Mejdahl, 1979), water content (81) and HF etching (83). Water contents were obtained using the modern measured water contents in most cases, but adjusted when evidence of modern drying of exposed sections was readily apparent (see SI p.5) For K-feldspar, internal grain K and Rb concentrations of 12.5 ± 0.5% and 400 ± 100 ppm respectively were assumed (84, 85). HF etching is assumed to have removed the α-irradiated outer portion of the quartz and (where used) feldspar grains. For the un-etched K feldspar samples an external alpha dose rate used an a-value of 0.15 ± 0.05 (86). Cosmic dose rates were determined using the measured sample depths in the "*Luminescence*" R package (77) and SI.

Hydrological modelling (SI p.56)

The Shetran hydrological model (31, 87) is physically-based, spatially-distributed and has a fully three-dimensional subsurface flow component. In Shetran there is an explicit representation of the groundwater and surface flows around and within the pan sites, including components for vegetation interception and transpiration, overland flow, variably saturated subsurface flow and channel-aquifer interactions. Solutions to the governing physics-based partial differential equations of mass and momentum are achieved on a three-dimensional grid using finite-difference equations (https://research.ncl.ac.uk/shetran/). The Orange River catchment was split into 28591 4 km x 4 km vertical columns. Each vertical column has an associated vegetation type on the ground surface and below ground is split into 35 cells, to 80 m below the ground surface, with small cells near the surface containing the soils and larger cells deeper below ground containing the aquifer. In addition, there are 1165 river channels that flow around the edge of the grid squares, automatically generated from the ground surface elevations (31).

Table S8 shows the original sources of spatial distributed data used by Shetran, which were aggregated up to a common 4 km resolution. The northwestern part of the basin is classed as being bare ground, the central part as shrubland and the eastern part as a mixture of arable and grassland. The bare ground corresponds to "Bushmanland", shrubland to "Upper Karoo" and "Eastern Kalahari Bushveld" and arable and grassland to "Dry Highveld Grassland", "Mesic Highveld Grassland" and "Drakensberg Grassland" (see vegetation reconstruction section, Fig. 59). Soils (Table S8) are generally well drained and either clay loams, sandy clay loams, sandy loams or sandy. Standard libraries were used for the soil and land-use parameter values (88). There is limited information about the aquifer properties within the catchment. As such, the same aquifer properties were applied throughout the model. Average spatially distributed monthly values of precipitation and potential evaporation were obtained from the WorldClim 2.1 dataset (89) and Global Aridity Index and Potential Evapotranspiration (ET0) Climate Database v2 (50). There is an increase in annual totals of precipitation going from west (<200 mm a^{-1}) to east (>1000 mm a^{-1}). Potential evaporation totals show a decrease from west (>1600 mm a^{-1}) to east (<1000 mm a^{-1}).

The aim of the hydrological simulation (outputs shown in Figs. S51, S53 and Table S9) was to produce the expected long-term water table and surface water depths, as observed and preserved at the lake basin study sites. The model was run for up to 100 years with the same annual precipitation and potential evaporation data until equilibrium conditions were achieved. Evapotranspiration is affected by the temporal distribution of the precipitation, so the monthly precipitation data were converted to daily precipitation using the expected number of wet days per month (https://www.fao.org/aquastat/en/geospatial-information/climate-information).

Palaeoecological analysis (SI p.61, 67)

To consider changes to vegetation and large ungulate resources associated with the inferred MIS 3-2 lacustrine periods we employed a modern analogue approach, based on the modern/historic distribution of biomes and bioregions (42) and fauna (43) and comparable climate data (50, 89).

The distribution of biomes in the interior is primarily determined by: 1) water availability (e.g. discriminating between Grassland and Nama-Karoo; Fig. S54) and 2) mean minimum temperature of the coldest month (TminColdM; a proxy for frost potential, e.g. discriminating between Grassland and Savanna; Fig. S54D) (47, 90). At the subcontinental scale, the seasonal distribution of rainfall is also significant, discriminating the winter-rainfall biomes of the Fynbos and Succulent Karoo of the southwestern Cape from the summer rainfall bioregions of the rest of southern Africa (Fig. S54C). Rainfall seasonality cannot be accurately quantified from the available proxy records, but our conclusions encompass the spectrum of vegetation types possible under the summer and winter-rainfall dominant scenarios. To estimate palaeotemperature during the lacustrine phases, we considered the proxy-based palaeo-temperature data available from southern Africa, which typically indicate a temperature depression of ~4-7°C at the Last Glacial Maximum (19-26.5 ka) (91), and an overall pattern that tracks global trends, as characterized by Antarctic ice core data (92). We used these patterns and data to create a temperature timeseries for the region, calibrated using regional temperature estimates (for amplitude of change) and the EPICA Antarctic temperature reconstruction (93) (for the timing of change) (92) (Fig. S56). Using these data, we established a temperature-based control on the potential influence of PET on the water balance during lacustrine phases, and then adjusted mean annual precipitation values to achieve the target P:PET ratios indicated by the Shetran hydrological model (Table S9). The MAP and PET data were used to calculate spatially continuous Aridity Index (AI) grids, the input values of which could be modified to reconstruct the water balance for the lacustrine phases in the South African interior.

To consider changes in regional fauna associated with MIS 2-3 environments, we re-analysed data from Equus Cave, the only faunal record from the South African interior that preserves remains dated to MIS 1, 2 and 3. The nature of the site's chronology does not permit detailed time series analyses, but it is sufficient to assess late Pleistocene assemblages (33, 94). For our analysis, we compared the large ungulates reported by Klein et al. (33) on a presence/absence basis with comparable modern/historic data compiled by Hempson et al. (43) for Sub-Saharan Africa (Fig. S60).

Acknowledgments

This work was funded by National Geographic Society grant CP-039R-17. The authors are grateful to landowners (Mr. Brandt, Mr. and Mrs. Barnard, De Beers) for providing land access, and the South African Heritage Resources Agency for support and guidance regarding permits. They also wish to thank David Morris (McGregor Museum) and Leon Jacobson (University of the Free State) for their assistance in relocating sites, Genevieve Tyrrell for conducting the stable isotope analyses, Adam Cox for performing the ICP-MS/ICP-OES analyses and Lynne Quick for her assistance in the field. The reviewers are also thanked for their very constructive comments.

References

1. Wadley L (2015) Those marvellous millennia: the Middle Stone Age of Southern Africa. *Azania: Archaeological Research in Africa* 50(2):155-226.
2. Klein RG*, et al.* (2004) The Ysterfontein 1 Middle Stone Age site, South Africa, and early human exploitation of coastal resources. *Proceedings of the National Academy of Sciences of the United States of America* 101(16):5708-5715.

3. Deacon HJ & Thackeray JF (1984) Late Pleistocene environmental changes and implications for the archaeological record in southern Africa. *Late Cainozoic Palaeoclimates of the Southern Hemisphere*, ed Vogel JC (Balkema, Rotterdam), pp 375-390.
4. Deacon HJ (1983) The Peopling of the Fynbos Region. *Fynbos palaeoecology: A preliminary synthesis*, eds Deacon HJ, Hendey QB, & Lambrechts JJN (Council for Scientific and Industrial Reseach, Pretoria, South Africa).
5. Parkington J (2010) Coastal Diet, Encephalization, and Innovative Behaviors in the Late Middle Stone Age of Southern Africa. *Human Brain Evolution: The Influence of Freshwater and Marine Food Resources*, eds Cunnane S & Stewart K (Wiley-Blackwell), pp 189-202.
6. Marean CW (2010) Pinnacle Point Cave 13B (Western Cape Province, South Africa) in context: The Cape Floral kingdom, shellfish, and modern human origins. *Journal of Human Evolution* 59(3-4):425-443.
7. Smith EI*, et al.* (2018) Humans thrived in South Africa through the Toba eruption about 74,000 years ago. *Nature* 555:511.
8. Marean CW (2010) When the Sea Saved Humanity. *Scientific American* 303(2):54-61.
9. Carr AS, Chase BM, & Mackay A (2016) Mid to Late Quaternary Landscape and Environmental Dynamics in the Middle Stone Age of Southern South Africa. *Africa from Stages 6-2: Population Dynamics an Palaeoenvironments,* Vertebrate Paleobiology and Paleoanthropology Series, eds Stewart BA & Jones S (Springer).
10. Burrough SL (2016) Late Quaternary Environmental Change and Human Occupation of the Southern African Interior. *Africa from MIS 6-2: Population Dynamics and Paleoenvironments*, eds Jones SC & Stewart BA (Springer Netherlands, Dordrecht), pp 161-174.
11. Wilkins J*, et al.* (2021) Innovative Homo sapiens behaviours 105,000 years ago in a wetter Kalahari. *Nature*.
12. von der Meden J*, et al.* (2022) Tufas indicate prolonged periods of water availability linked to human occupation in the southern Kalahari. *PLOS ONE* 17(7):e0270104.
13. Coulson S*, et al.* (2022) Thriving in the Thirstland: New Stone Age sites from the Middle Kalahari, Botswana. *Quaternary Science Reviews* 297:107695.
14. Beaumont PB (1986) Where did all the young men go during ^{18}O stage 2? *Palaeoecology of Africa* 17:79-86.
15. Hallinan E (2021) Landscape-scale perspectives on Stone Age behavioural change from the Tankwa Karoo, South Africa. *Azania: Archaeological Research in Africa*:1-40.
16. Wroth K*, et al.* (2022) Human occupation of the semi-arid grasslands of South Africa during MIS 4: New archaeological and paleoecological evidence from Lovedale, Free State. *Quaternary Science Reviews* 283:107455.
17. Kaboth-Bahr S*, et al.* (2021) Paleo-ENSO influence on African environments and early modern humans. *Proceedings of the National Academy of Sciences* 118(23):e2018277118.
18. Blome MW, Cohen AS, Tryon CA, Brooks AS, & Russell J (2012) The environmental context for the origins of modern human diversity: A synthesis of regional variability in African climate 150,000–30,000 years ago. *Journal of Human Evolution* 62(5):563-592.
19. Groucutt HS*, et al.* (2021) Multiple hominin dispersals into Southwest Asia over the past 400,000 years. *Nature*.

20. Cohen TJ*, et al.* (2012) Late Quaternary mega-lakes fed by the northern and southern river systems of central Australia: Varying moisture sources and increased continental aridity. *Palaeogeography, Palaeoclimatology, Palaeoecology* 356–357(0):89-108.
21. Burrough SL, Thomas DSG, & Bailey RM (2009) Mega-Lake in the Kalahari: a late Pleistocene record of the Palaeolake Makgadikgadi system. *Quaternary Science Reviews* 28(15-16):1392-1411.
22. Ibarra DE, Egger AE, Weaver KL, Harris CR, & Maher K (2014) Rise and fall of late Pleistocene pluvial lakes in response to reduced evaporation and precipitation: Evidence from Lake Surprise, California. *GSA Bulletin* 126(11-12):1387-1415.
23. Kent LE & Gribnitz KH (1985) Fresh-water shell deposits in the northwestern Cape Province: further evidence for a widespread wet phase during the Late Pleistocene in southern Africa. *South African Journal of Science* 81(7):361-370.
24. Butzer KW, Fock GJ, Stuckenrath R, & Zilch A (1973) Paleohydrology of Late Pleistocene Lake Alexandersfontein, Kimberley, South Africa. *Nature* 243:328-330.
25. Kiberd P & Pryor A (2021) *Ostrich eggshell isotope data from Bundu Farm, South Africa, and new evidence on middle stone age environments in the upper Karoo* (South African Archaeological Society) pp 31–42.
26. Sampson CG (1985) *Atlas of Stone Age settlement in the central and upper Seacow valley* (Bloemfontein).
27. Wallsmith DL (1994) Lithic management strategies of Late Middle Stone Age hunter-gatherers in the upper Karoo region of South Africa. PhD (Southern Methodist University).
28. Leng MJ & Marshall JD (2004) Palaeoclimate interpretation of stable isotope data from lake sediment archives. *Quaternary Science Reviews* 23(7-8):811-831.
29. Sonamzi B, Mlambo MC, Appleton CC, & Barber-James HM (2019) The importance of museum collections in determining biodiversity patterns, using a freshwater mussel Unio caffer (Krauss 1848) as an example. *Bothalia - African Biodiversity & Conservation* 49:1-7.
30. Butzer KW (1984) Archeogeology and Quaternary environment in the interior of southern Africa. *Southern African prehistory and paleoenvironments*, ed Klein RG (Balkema), pp 1-64.
31. Birkinshaw SJ, James P, & Ewen J (2010) Graphical user interface for rapid set-up of SHETRAN physically-based river catchment model. *Environmental Modelling & Software* 25(4):609-610.
32. Butzer KW, Helgren DM, Fock GJ, & Stuckenrath R (1973) Alluvial Terraces of the Lower Vaal River, South Africa: A Reappraisal and Reinvestigation. *The Journal of Geology* 81(3):341-362.
33. Klein RG, Cruz-Uribe K, & Beaumont PB (1991) Environmental, ecological, and paleoanthropological implications of the Late Pleistocene mammalian fauna from Equus Cave, northern Cape Province, South Africa. *Quaternary Research* 36(1):94-119.
34. Brook GA, Scott L, Railsback LB, & Goddard EA (2010) A 35 ka pollen and isotope record of environmental change along the southern margin of the Kalahari from a stalagmite and animal dung deposits in Wonderwerk Cave, South Africa. *Journal of Arid Environments* 74(7):870-884.

35. Holmgren K, Karlen W, & Shaw PA (1995) Paleoclimatic significance of the stable isotopic composition and petrology of a Late Pleistocene stalagmite from Botswana. *Quaternary Research* 43(3):320-328.
36. Chase BM*, et al.* (2021) South African speleothems reveal influence of high- and lowlatitude forcing over the past 113.5 k.y. *Geology*.
37. Fischer H*, et al.* (2007) Reconstruction of millennial changes in dust emission, transport and regional sea ice coverage using the deep EPICA ice cores from the Atlantic and Indian Ocean sector of Antarctica. *Earth and Planetary Science Letters* 260(1–2):340-354.
38. Todd M & Washington R (1999) Circulation anomalies associated with tropical-temperate troughs in southern Africa and the south west Indian Ocean. *Climate Dynamics* 15(12):937-951.
39. Chase BM, Chevalier M, Boom A, & Carr AS (2017) The dynamic relationship between temperate and tropical circulation systems across South Africa since the last glacial maximum. *Quaternary Science Reviews* 174:54-62.
40. Lee-Thorp JA & Beaumont PB (1995) Vegetation and seasonality shifts during the late Quaternary deduced from $^{13}C/^{12}C$ ratios of grazers at Equus Cave, South Africa. *Quaternary Research* 43(3 SU -):426-432.
41. Holmgren K, Lauritzen SE, & Possnert G (1994) Th-230/U-234 and C-14 dating of a Late Pleistocene stalagmite in Lobatse-II Cave, Botswana. *Quaternary Science Reviews* 13(2):111-119.
42. Mucina L & Rutherford MC eds (2006) *The vegetation of South Africa, Lesotho and Swaziland* (South African National Biodiversity Institute, Pretoria), Vol 19.
43. Hempson GP, Archibald S, & Bond WJ (2015) A continent-wide assessment of the form and intensity of large mammal herbivory in Africa. *Science* 350(6264):1056-1061.
44. Mucina L*, et al.* (2006) Grassland Biome. *The Vegetation of South Africa, Lesotho and Swaziland*, eds Mucina L & Rutherford MC (South African National Biodiversity Institute, Pretoria), pp 349-436.
45. Hoare DB & Bredenkamp GJ (2001) Syntaxonomy and environmental gradients of the grasslands of the Stormberg / Drakensberg mountain region of the Eastern Cape, South Africa. *South African Journal of Botany* 67(4):595-608.
46. Ellery WN, Scholes RJ, & Scholes MC (1995) The distribution of sweetveld and sourveld in South Africa's grassland biome in relation to environmental factors. *African Journal of Range & Forage Science* 12(1):38-45.
47. Rutherford MC (1997) Categorization of biomes. *Vegetation of Southern Africa*, eds Cowling RM, Richardson DM, & Pierce SM (Cambridge University Press).
48. Scott L (1987) Pollen analysis of hyena coprolites and sediments from Equus Cave, Taung, southern Kalahari (South Africa). *Quaternary Research* 28(1):144-156.
49. Rutherford MC*, et al.* (2006) Savanna Biome. *The Vegetation of South Africa, Lesotho and Swaziland*, eds Mucina L & Rutherford MC (South African National Biodiversity Institute, Pretoria), pp 439-538.
50. Trabucco A & Zomer R (2019) Global Aridity Index and Potential Evapotranspiration (ET0) Climate Database v2. ed figshare.
51. Scott L*, et al.* (2019) Palynology of Middle Stone Age spring deposits in grassland at the Florisbad hominin site, South Africa. *Review of Palaeobotany and Palynology* 265:13-26.

52. Brink JS (1987) *The archaeozoology of Florisbad, Orange Free State* (National Museum, Bloemfontein).
53. Marean CW, Cowling RM, & Franklin J (2020) The Palaeo-Agulhas Plain: Temporal and spatial variation in an extraordinary extinct ecosystem of the Pleistocene of the Cape Floristic Region. *Quaternary Science Reviews* 235:106161.
54. Mitchell P (2008) Developing the archaeology of marine isotope stage 3. *Goodwin Series* 10:52-65.
55. Sampson CG*, et al.* (2015) A GIS Analysis of the Zeekoe Valley Stone Age Archaeological Record in South Africa. *Journal of African Archaeology* 13(2):167-185.
56. Stewart BA, Parker AG, Dewar G, Morley MW, & Allott LF (2016) Follow the Senqu: Maloti-Drakensberg paleoenvironments and implications for early human dispersals into mountain systems. *Africa from MIS 6-2*, eds Jones SC & Stewart BA (Springer, Dordrecht), pp 247-271.
57. Butzer KW (1988) Sedimentological interpretation of the Florisbad spring deposits, South Africa. *Palaeoecology of Africa* 19:181-189.
58. Butzer KW (1988) A marginality model to explain major spatial and temporal gaps in the old and new world Pleistocene settlement records. *Geoacrchaeology* 3(3):193-203.
59. Roberts P & Stewart BA (2018) Defining the 'generalist specialist' niche for Pleistocene Homo sapiens. *Nature Human Behaviour* 2(8):542-550.
60. Mackay A*, et al.* (2022) Environmental influences on human innovation and behavioural diversity in southern Africa 92–80 thousand years ago. *Nature Ecology & Evolution*.
61. Mackay A, Stewart BA, & Chase BM (2014) Coalescence and fragmentation in the late Pleistocene archaeology of southernmost Africa. *Journal of Human Evolution* 72(0):26-51.
62. Pargeter J (2016) Lithic miniaturization in Late Pleistocene southern Africa. *Journal of Archaeological Science: Reports* 10:221-236.
63. Stewart BA*, et al.* (2020) Ostrich eggshell bead strontium isotopes reveal persistent macroscale social networking across late Quaternary southern Africa. *Proceedings of the National Academy of Sciences*:201921037.
64. Chazan M*, et al.* (2020) Archeology, Environment, and Chronology of the Early Middle Stone Age Component of Wonderwerk Cave. *Journal of Paleolithic Archaeology* 3(3):302-335.
65. Burrough SL*, et al.* (2022) Lessons from a lakebed: unpicking hydrological change and early human landscape use in the Makgadikgadi basin, Botswana. *Quaternary Science Reviews*:107662.
66. Thomas DSG*, et al.* (2022) Lacustrine geoarchaeology in the central Kalahari: Implications for Middle Stone Age behaviour and adaptation in dryland conditions. *Quaternary Science Reviews* 297:107826.
67. Yamazaki D*, et al.* (2017) A high-accuracy map of global terrain elevations. *Geophysical Research Letters* 44(11):5844-5853.
68. Stuiver M, Reimer PJ, & Reimer RW (2021) CALIB), 8.1.
69. Hogg AG*, et al.* (2020) SHCal20 Southern Hemisphere Calibration, 0–55,000 years cal BP. *Radiocarbon*:1-20.
70. Wintle AG (1997) Luminescence dating: laboratory procedures and protocols. *Radiation Measurements* 27(5-6):769-817.

71. Murray AS & Wintle AG (2000) Luminescence dating of quartz using an improved single-aliquot regenerative-dose protocol. *Radiation Measurements* 32(1):57-73.
72. Murray AS & Wintle AG (2003) The single aliquot regenerative dose protocol: potential for improvements in reliability. *Radiation Measurements* 37(4-5):377-381.
73. Buylaert JP, Murray AS, Thomsen KJ, & Jain M (2009) Testing the potential of an elevated temperature IRSL signal from K-feldspar. *Radiation Measurements* 44(5):560-565.
74. Buylaert J-P*, et al.* (2012) A robust feldspar luminescence dating method for Middle and Late Pleistocene sediments. *Boreas* 41(3):435-451.
75. Thomsen KJ, Murray AS, Jain M, & Bøtter-Jensen L (2008) Laboratory fading rates of various luminescence signals from feldspar-rich sediment extracts. *Radiation Measurements* 43:1474-1486.
76. Auclair M, Lamothe M, & Huot S (2003) Measurement of anomalous fading for feldspar IRSL using SAR. *Radiation Measurements* 37(4):487-492.
77. Kreutzer S*, et al.* (2023) Luminescence: Comprehensive Luminescence Dating Data Analysis), 0.9.21.
78. Jacobs Z, Duller GAT, & Wintle AG (2006) Interpretation of single grain De distributions and calculation of De. *Radiation Measurements* 41(3):264-277.
79. Martinón-Torres M*, et al.* (2021) Earliest known human burial in Africa. *Nature* 593(7857):95-100.
80. Jacobs Z & Roberts RG (2015) An improved single grain OSL chronology for the sedimentary deposits from Diepkloof Rockshelter, Western Cape, South Africa. *Journal of Archaeological Science* 63:175-192.
81. Aitken MJ (1985) *Thermoluminescence Dating* (Academic Press, London and New York) p 359.
82. Guérin G, Mercier N, & Adamiec G (2011) Dose-rate conversion factors: update. *Ancient TL* 29(1):5-8.
83. Bell WT (1979) Thermoluminescence dating: radiation dose-rate data. *Archaeometry* 21(2):243-245.
84. Huntley DJ & Baril MR (1997) The K content of the K-feldspars being measured in optical dating or in thermoluminescence dating. *Ancient TL* 15:11-13.
85. Huntley DJ & Hancock RGV (2001) The Rb contents of the K-feldspar grains being measured in optical dating. *Ancient TL* 19:43-46.
86. Balescu S & Lamothe M (1993) Thermoluminescence dating of the holsteinian marine formation of Herzeele, northern France. *Journal of Quaternary Science* 8(2):117-124.
87. Ewen J, Parkin G, & O'Connell PE (2000) SHETRAN: Distributed River Basin Flow and Transport Modeling System. *Journal of Hydrologic Engineering* 5(3):250-258.
88. Lewis E, Birkinshaw S, Kilsby C, & Fowler HJ (2018) Development of a system for automated setup of a physically-based, spatially-distributed hydrological model for catchments in Great Britain. *Environmental Modelling & Software* 108:102-110.
89. Fick SE & Hijmans RJ (2017) WorldClim 2: new 1-km spatial resolution climate surfaces for global land areas. *International Journal of Climatology* 37(12):4302-4315.
90. Ellery MT, W.N. S, R.J., & Mentis (1991) An initial approach to predicting the sensitivity of the South African grassland biome to climate change. *South African Journal of Science* 87(10):499-503.

91. Chevalier M & Chase BM (2015) Southeast African records reveal a coherent shift from high- to low-latitude forcing mechanisms along the east African margin across last glacial–interglacial transition. *Quaternary Science Reviews* 125:117-130.
92. Chevalier M, Chase BM, Quick LJ, Dupont LM, & Johnson TC (2020) Temperature change in subtropical southeastern Africa during the past 790,000 yr. *Geology*.
93. Jouzel J*, et al.* (2007) Orbital and millennial Antarctic climate variability over the past 800,000 years. *Science* 317:793-797.
94. Scott L*, et al.* (2020) Late Quaternary palaeoenvironments in the central semi-arid region of South Africa from pollen in cave, pan, spring, stream and dung deposits. *Quaternary International*.
95. Laskar J*, et al.* (2004) A long-term numerical solution for the insolation quantities of the Earth. *A&A* 428(1):261-285.
96. Partridge TC, deMenocal PB, Lorentz SA, Paiker MJ, & Vogel JC (1997) Orbital forcing of climate over South Africa: a 200,000-year rainfall record from the Pretoria Saltpan. *Quaternary Science Reviews* 16(10):1125-1133.
97. Braun K*, et al.* (2020) Comparison of climate and environment on the edge of the Palaeo-Agulhas Plain to the Little Karoo (South Africa) in Marine Isotope Stages 5–3 as indicated by speleothems. *Quaternary Science Reviews* 235:105803.

Figure captions

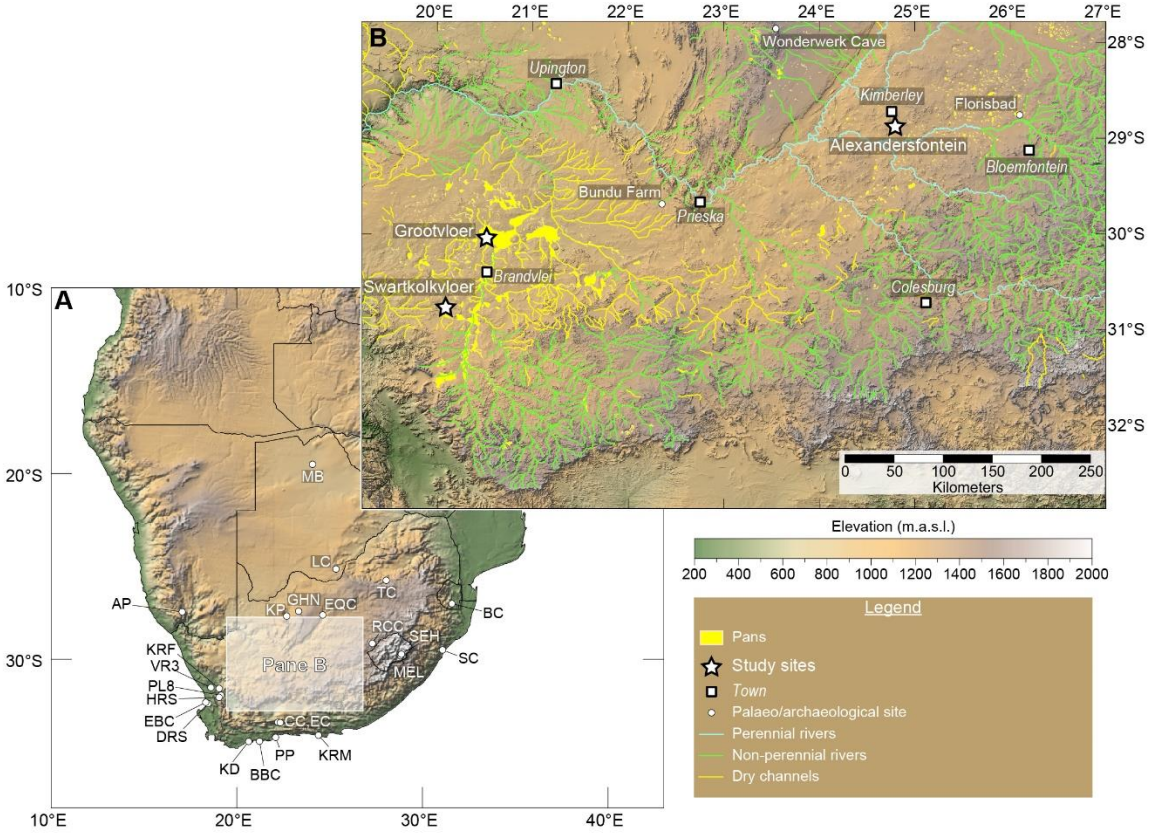

Fig. 1: Map of South African study region with modern hydrologic system, study sites and relevant paleoenvironmental and archaeological sites. Site codes indicated are as follows: AP = Apollo 11 Rockshelter; BBC = Blombos Cave; BC = Border Cave; CC = Cango Cave; DK = Die Kelders Cave; DRS = Diepkloof Rockshelter; EBC = Elands Bay Cave; EC = Efflux Cave; EQC = Equus Cave; GHN = Ga Mohana Rockshelter; HRS = Hollow Rock Shelter; KD = Klipdrift Cave; KFR = Klipfonteinrand; KP = Kathu Pan; KRM = Klasies River Mouth; Lobatse Cave = LC; MB = Makgadikgadi Basin; MEL = Melikane Rockshelter; PP = Pinnacle Point sites; PL8 = Putslaagte 8; RCC = Rose Cottage Cave; SC = Sibudu Cave; SEH = Sehonghong Rockshelter; TC = Tswaing Crater; VR3 = Varsche River 3.

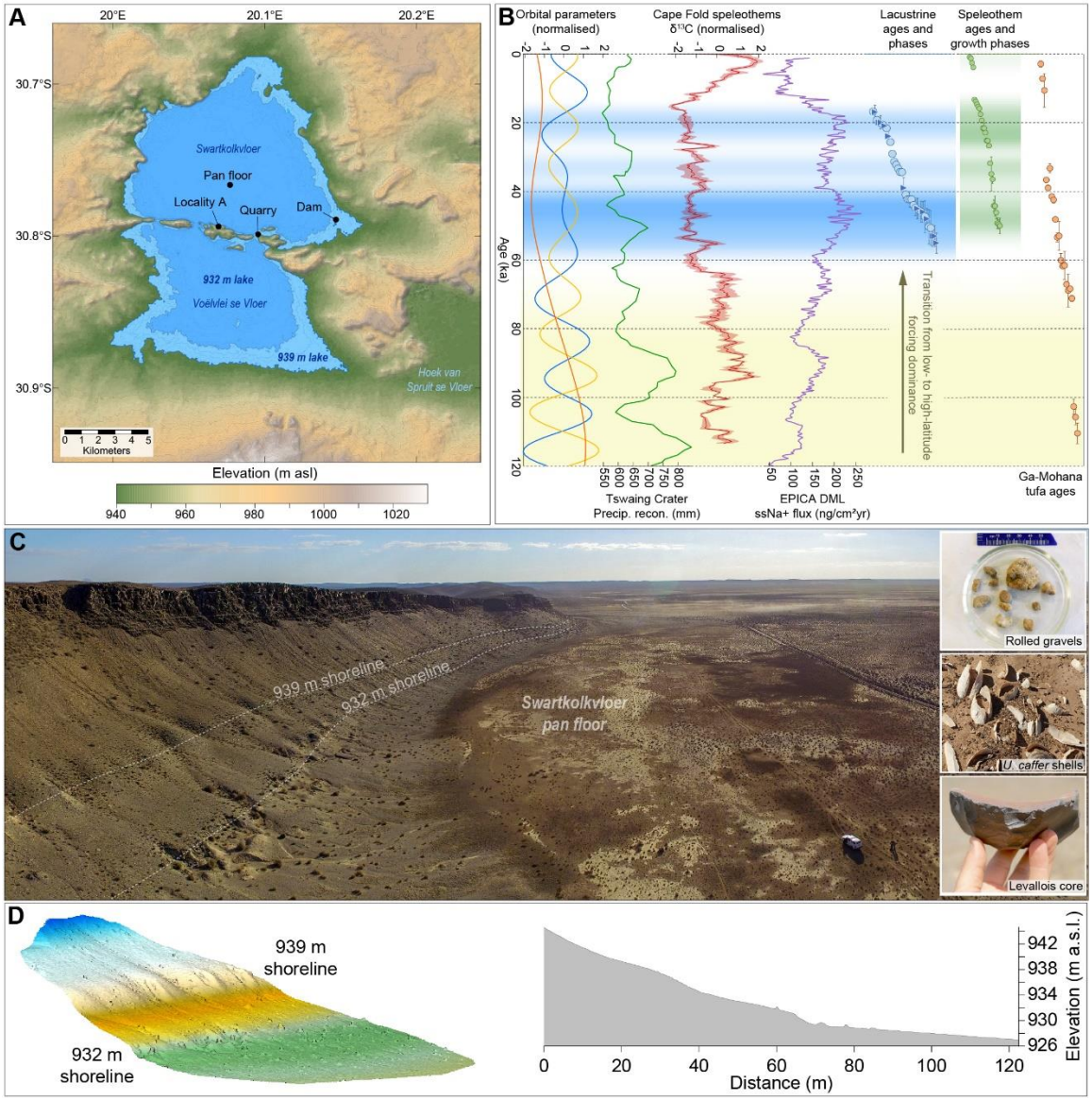

Fig. 2. Map of Swartkolkvloer (A) with specific and summary data indicating lacustrine phases. View of Swartkolkvloer (B, from east) indicating the upper and lower shorelines (rendered in a photogrammetric model and derived slope profile (D)) and the locations of the sampling sites. Examples of evidence for sustained lacustrine conditions in the form of rolled gravel and freshwater molluscs are shown to the right of pane B, as is a Levallois core found along the lower shoreline. Pane C provides a comparison of optically-stimulated luminescence (triangles) and ^{14}C (circles) ages obtained from lacustrine materials as part of this study from the South African interior (blue) with orbital parameters (95), the Tswaing Crater precipitation reconstruction (96), speleothem $\delta^{13}C$ data from the Cape Fold mountains (36, 97) indicating the transition to cooler glacial conditions, the EPICA DML sea-salt Na flux as a proxy for Antarctic sea-ice (37), and interpolated speleothem growth ages from Wonderwerk (34) and Lobatse (35) caves. Yellow shading indicates transition from low to high latitude forcing dominance as inferred from regional data (36).

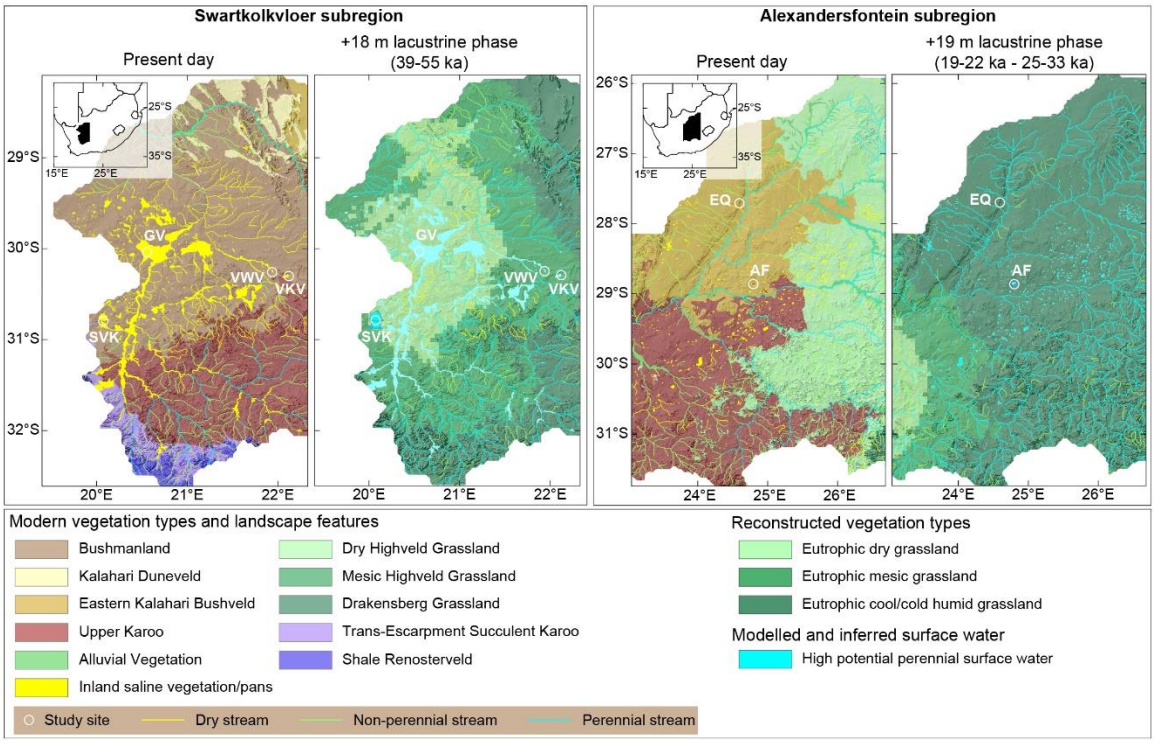

Fig. 3: Present-day conditions and environmental reconstructions for lacustrine phases. Maps of western and eastern subregions of the Orange and Vaal river catchments of the South African interior depicting present day hydrologic networks and vegetation bioregions as compared to hydrologies and vegetation types likely associated with key lacustrine phases identified in the geological record.